Multinucleon transfer in central collisions of ^{238}U + ^{238}U

S. Ayik,[1,*] B. Yilmaz,[2] O. Yilmaz,[3] A. S. Umar,[4] and G. Turan[3]
[1]*Physics Department, Tennessee Technological University, Cookeville, Tennessee 38505, USA*
[2]*Physics Department, Faculty of Sciences, Ankara University, 06100 Ankara, Turkey*
[3]*Physics Department, Middle East Technical University, 06800 Ankara, Turkey*
[4]*Department of Physics and Astronomy, Vanderbilt University, Nashville, Tennessee 37235, USA*
(Received 12 June 2017; published 14 August 2017)

Quantal diffusion mechanism of nucleon exchange is studied in the central collisions of ^{238}U + ^{238}U in the framework of the stochastic mean-field (SMF) approach. For bombarding energies considered in this work, the dinuclear structure is maintained during the collision. Hence, it is possible to describe nucleon exchange as a diffusion process for mass and charge asymmetry. Quantal neutron and proton diffusion coefficients, including memory effects, are extracted from the SMF approach and the primary fragment distributions are calculated.

DOI: 10.1103/PhysRevC.96.024611

I. INTRODUCTION

Recently, much work has been done to investigate the multinucleon transfer processes in heavy-ion collisions near barrier energies. For this purpose, the quasifission reaction of heavy ions provides an important tool. The colliding ions are attached together for a long time, but separate without going through compound nucleus formation. During the long contact times many nucleon exchanges take place between projectile and target nuclei. A number of models was developed for a description of the reaction mechanism in the multinucleon transfer process in quasifission reactions [1–4]. Within the last few years the time-dependent Hartree-Fock (TDHF) approach [5–7] has been utilized for studying the dynamics of quasifission [7–17] and scission dynamics [18–23]. Such calculations are now numerically feasible to perform on a three-dimensional (3D) Cartesian grid without any symmetry restrictions and with much more accurate numerical methods [24–26].

The mean-field description of reactions using TDHF provides the mean values of the proton and neutron drift. It is also possible to compute the probability to form a fragment with a given number of nucleons [27–32], but the resulting fragment mass and charge distributions are often underestimated in dissipative collisions [33,34]. Much effort has been done to improve the standard mean-field approximation by incorporating the fluctuation mechanism into the description. At low energies, the mean-field fluctuations make the dominant contribution to the fluctuation mechanism of the collective motion. Various extensions have been developed to study the fluctuations of one-body observables. These include the TDRPA approach of Balian and Vénéroni [35], the time-dependent generator coordinate method [36], or the stochastic mean-field (SMF) method [37]. The effects of two-body dissipation on reactions of heavy systems using the TDDM [38,39], approach have also been recently reported [40,41]. Here we discuss some recent results using the SMF method [42].

In the SMF approach dynamical description is extended beyond the standard approximation by incorporating the mean-field fluctuations into the description [37]. In a number of studies, it has been demonstrated that the SMF approach is a good remedy for this shortcoming of the mean-field approach and improves the description of the collisions dynamics by including fluctuation mechanism of the collective motion [42–45]. Most applications have been carried out in collisions where a dinuclear structure is maintained. In this case, it is possible to define macroscopic variables with the help of the window dynamics. The SMF approach gives rise to a Langevin description for the evolution of macroscopic variables [46,47] and provides a microscopic basis to calculate transport coefficients for the macroscopic variables. In most application, this approach has been applied to the nucleon diffusion mechanism in the semiclassical limit and by ignoring the memory effects. In a recent work, we were able to deduce the quantal diffusion coefficients for nucleon exchange in the central collisions of heavy ions [48] from the SMF approach. The quantal transport coefficients include the effect of shell structure, take into account the full geometry of the collision process, and incorporate the effect of Pauli blocking exactly. We applied the quantal diffusion approach and carried out calculations for the variance of neutron and proton distributions of the outgoing fragments in the central collisions of several symmetric heavy-ion systems at bombarding energies slightly below the fusion barriers [48]. In this work we carry out quantal nucleon diffusion calculations and determine the primary fragment mass and charge distributions in the central collisions of ^{238}U + ^{238}U system in side-side and tip-tip configurations. Since the presented calculations do not involve any fitting parameters, the results may provide a useful guidance for the experimental investigations of heavy neutron rich isotopes originating from these reactions.

In Sec. II, we present a brief description of the quantal nucleon diffusion mechanism based on the SMF approach. In Sec. III, we present a brief discussion of quantal neutron and proton diffusion coefficients. The result of calculations is reported in Sec. IV, and conclusions are given in Sec. V.

*ayik@tntech.edu

II. NUCLEON DIFFUSION DESCRIPTION

In heavy-ion collisions when the system maintains a binary structure, the reaction evolves mainly due to nucleon exchange through the window between the projectile-like and target-like partners. It is possible to analyze nucleon exchange mechanism by employing nucleon diffusion concept based on the SMF approach. In the SMF approach, the standard mean-field description is extended by incorporating the mean-field fluctuations in terms of generating an ensemble of events according to quantal and thermal fluctuations in the initial state. Instead of following a single path, in the SMF approach dynamical evolution is determined by an ensemble of Slater determinants. The initial conditions of the single-particle density matrices associated with the ensemble Slater determinants are specified in terms of the quantal and thermal fluctuations of the initial state. For a detailed description of the SMF approach, we refer to [37,42–44]. In extracting transport coefficients for nucleon exchange, we take the proton and neutron numbers of projectile-like fragments Z_1^λ, N_1^λ as independent variables, where λ indicates the event label. We can define the proton and neutron numbers of the projectile-like fragments in each event by integrating over the nucleon density on the projectile side of the window. In the central collisions of symmetric systems, the window is perpendicular to the collision direction taken as the x axis and the position of the window is fixed at the origin of the center of mass frame according to the mean-field description of the TDHF. The proton and neutron numbers of the projectile-like fragments in each events are defined as

$$\begin{pmatrix} Z_1^\lambda(t) \\ N_1^\lambda(t) \end{pmatrix} = \int d^3r\theta(x - x_0) \begin{pmatrix} \rho_p^\lambda(\vec{r},t) \\ \rho_n^\lambda(\vec{r},t) \end{pmatrix}. \quad (1)$$

Here, $x_0 = 0$ denotes average position of the window plane taken as the origin of the center of mass frame and $\rho_p^\lambda(\vec{r},t)$ and $\rho_n^\lambda(\vec{r},t)$ are the local densities of protons and neutrons. Nucleon diffusion description, developed from the SMF approach in Ref. [48], is suitable for collisions in which a dinuclear structure is maintained during the entire reaction. There is a range of low bombarding energies in which dinuclear structure is maintained in $^{238}\mathrm{U} + ^{238}\mathrm{U}$ collisions for different geometric orientations. In our work, we carry out the calculations at $E_{\mathrm{c.m.}} = 900$ MeV and $E_{\mathrm{c.m.}} = 1050$ MeV for the side-side and tip-tip configurations, respectively. Figure 1 shows the evolution of the average density profiles in the side-side and tip-tip configurations in these collisions. In the calculation of this figure and in the calculations presented in the rest of the article, we employ the TDHF code developed by Umar *et al.* [24,49] using the SLy4d Skyrme functional [50].

In the collision of symmetric systems, location of the window plane remains stationary, and on the average, there is no net nucleon transfer between projectile and target nuclei. According to the SMF approach, the proton and neutron numbers of the projectile-like fragment follows a stochastic evolution according to the Langevin equations,

$$\frac{d}{dt}\begin{pmatrix} Z_1^\lambda(t) \\ N_1^\lambda(t) \end{pmatrix} = \int d^3r g(x) \begin{pmatrix} J_p^\lambda(\vec{r},t) \\ J_n^\lambda(\vec{r},t) \end{pmatrix} = \begin{pmatrix} v_p^\lambda(t) \\ v_n^\lambda(t) \end{pmatrix}. \quad (2)$$

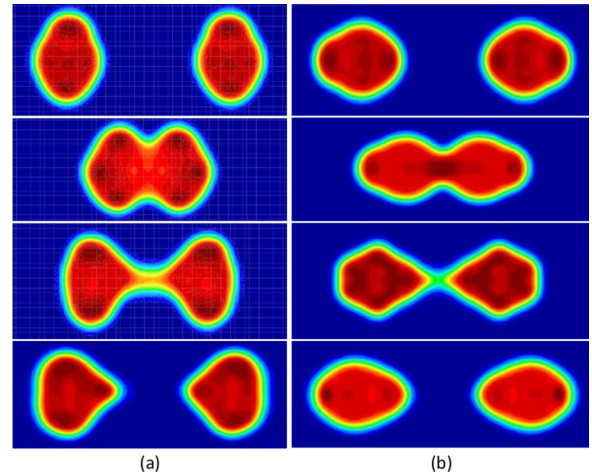

FIG. 1. Density profiles in the reaction plane in the central collisions of $^{238}\mathrm{U} + ^{238}\mathrm{U}$ (a) side-side collision with energy $E_{\mathrm{c.m.}} =$ 900 MeV from top to bottom at times $t = 0$, 400, 800, and 950 fm/c, and (b) tip-tip collision with energy $E_{\mathrm{c.m.}} = 1050$ MeV from top to bottom at times $t = 0$, 200, 700, and 800 fm/c, respectively, obtained in TDHF calculations.

In this expression, in place of the δ function $\delta(x)$ we introduce a Gaussian smoothing function $g(x)$ for convenience,

$$g(x) = \frac{1}{\sqrt{2\pi\kappa^2}} \exp\left(-\frac{x^2}{2\kappa^2}\right), \quad (3)$$

which approaches the δ function $\delta(x)$ in the limit $\kappa \to 0$. For the smoothing parameter, we take the value $\kappa = 1$ fm. This value is in the order of lattice spacing of the numerical calculations performed in this work. The right-hand side of Eq. (2) denotes the proton $v_p^\lambda(t)$ and neutron $v_n^\lambda(t)$ drift coefficients in the event λ, which are determined by the proton and the neutron current densities, $J_p^\lambda(\vec{r},t)$ and $J_n^\lambda(\vec{r},t)$, through the window in that event. In the SMF approach, the fluctuating proton and neutron currents densities in the collision direction are determined to be

$$J_\alpha^\lambda(\vec{r},t) = \frac{\hbar}{m} \sum_{ij\in\alpha} \mathrm{Im}(\Phi_j^*(\vec{r},t;\lambda)\nabla_x \Phi_i(\vec{r},t;\lambda))\rho_{ji}^\lambda. \quad (4)$$

Here, and in the rest of the paper, we use the label $\alpha = p,n$ for the proton and neutron states. In the description of the SMF approach, the elements of density matrices ρ_{ji}^λ are taken as uncorrelated Gaussian numbers. The mean values of the elements of density matrices are given by $\overline{\rho}_{ji}^\lambda = \delta_{ji} n_j$ and the second moments of fluctuating parts are determined by

$$\overline{\delta\rho_{ji}^\lambda \delta\rho_{i'j'}^\lambda} = \tfrac{1}{2}\delta_{ii'}\delta_{jj'}[n_i(1-n_j) + n_j(1-n_i)], \quad (5)$$

where n_j are the average occupation numbers of the single-particle states.

For small amplitude fluctuations, by taking the ensemble averaging, we obtain the usual mean-field result given by the

TDHF equations

$$\frac{d}{dt}\begin{pmatrix} Z_1(t) \\ N_1(t) \end{pmatrix} = \int d^3r g(x) \begin{pmatrix} J_p(\vec{r},t) \\ J_n(\vec{r},t) \end{pmatrix} = \begin{pmatrix} v_p(t) \\ v_n(t) \end{pmatrix}. \quad (6)$$

Here, $Z_1 = \overline{Z}_1^{\lambda}$, $N_1 = \overline{N}_1^{\lambda}$, $J_\alpha(\vec{r}) = \overline{J}_\alpha^{\lambda}(\vec{r})$, and $v_\alpha = \overline{v}_\alpha^{\lambda}$ indicate the mean values of the proton and neutron numbers of projectile-like fragments, proton and neutron current densities, and proton and neutron drift coefficients, which are average values taken over the ensemble single-particle densities. Mean values of the current densities of protons and neutrons along the collision direction are given by

$$J_\alpha(\vec{r},t) = \frac{\hbar}{m}\sum_{h\in\alpha} \mathrm{Im}(\Phi_h^*(\vec{r},t)\nabla_x \Phi_h(\vec{r},t)), \quad (7)$$

where the summation h runs over the occupied states originating both from the projectile and the target nuclei. Drift coefficients $v_p^\lambda(t)$ and $v_n^\lambda(t)$ fluctuate from event to event due to stochastic elements of the initial density matrix ρ_{ji}^λ and also due to the different sets of the wave functions in different events. As a result, there are two sources for fluctuations of the nucleon current: (i) fluctuations those arise from the state dependence of the drift coefficients, which may be approximately represented in terms of fluctuations of proton and neutron partition of the dinuclear system, and (ii) the explicit fluctuations $\delta v_p^\lambda(t)$ and $\delta v_n^\lambda(t)$ which arise from the stochastic part of proton and neutron currents. For small amplitude fluctuations, we can linearize the Langevin Eq. (2) around the mean evolution to obtain

$$\frac{d}{dt}\begin{pmatrix} \delta Z_1^\lambda(t) \\ \delta N_1^\lambda(t) \end{pmatrix} = \begin{pmatrix} \frac{\partial v_p}{\partial Z_1}(Z_1^\lambda - Z_1) + \frac{\partial v_p}{\partial N_1}(N_1^\lambda - N_1) \\ \frac{\partial v_n}{\partial Z_1}(Z^\lambda - Z_1) + \frac{\partial v_n}{\partial N_1}(N_1^\lambda - N_1) \end{pmatrix} + \begin{pmatrix} \delta v_p^\lambda(t) \\ \delta v_n^\lambda(t) \end{pmatrix}. \quad (8)$$

The variances and the covariance of neutron and proton distribution of projectile fragments are defined as $\sigma_{NN}^2(t) = \overline{(N_1^\lambda - N_1)^2}$, $\sigma_{ZZ}^2(t) = \overline{(Z_1^\lambda - Z_1)^2}$, and $\sigma_{NZ}^2(t) = \overline{(N_1^\lambda - N_1)(Z_1^\lambda - Z_1)}$. Multiplying both sides of Eq. (8) by $N_1^\lambda - N_1$ and $Z_1^\lambda - Z_1$, and taking the ensemble average, it is possible to obtain set of coupled differential equations for the covariances [51,52]. These differential equations are given by

$$\frac{\partial}{\partial t}\sigma_{NN}^2 = 2\frac{\partial v_n}{\partial N_1}\sigma_{NN}^2 + 2\frac{\partial v_n}{\partial Z_1}\sigma_{NZ}^2 + 2D_{NN}, \quad (9)$$

$$\frac{\partial}{\partial t}\sigma_{ZZ}^2 = 2\frac{\partial v_p}{\partial Z_1}\sigma_{ZZ}^2 + 2\frac{\partial v_p}{\partial N_1}\sigma_{NZ}^2 + 2D_{ZZ}, \quad (10)$$

$$\frac{\partial}{\partial t}\sigma_{NZ}^2 = \frac{\partial v_p}{\partial N_1}\sigma_{NN}^2 + \frac{\partial v_n}{\partial Z_1}\sigma_{ZZ}^2 + \sigma_{NZ}^2\left(\frac{\partial v_p}{\partial Z_1} + \frac{\partial v_n}{\partial N_1}\right). \quad (11)$$

Here, D_{NN} and D_{ZZ} indicate the diffusion coefficients of proton and neutron exchanges. In order to determine the covariances in addition to the diffusion coefficients, we need to know derivatives of drift coefficients with respect to the proton and neutron numbers. These derivatives are evaluated at the mean values of the neutron and proton numbers. In symmetric collisions, mean values of the drift coefficients are zero, but in general, their slopes at the zero mean values do not vanish.

It is well know that the Langevin description is equivalent to the Fokker-Planck description of the probability distribution function $P(N,Z,t)$ primary fragments as a function of the neutron and proton numbers [53]. When fluctuating drift coefficients are linear functions of the fluctuating proton and neutron numbers, the probability distribution of the project-like or the target-like fragments are specified by a correlated Gaussian function,

$$P(N,Z,t) = \frac{1}{2\pi\sigma_{NN}\sigma_{ZZ}\sqrt{1-\rho^2}}\exp(-C). \quad (12)$$

Here, the exponent C is given by

$$C = \frac{1}{2(1-\rho^2)}\left[\left(\frac{Z-\overline{Z}}{\sigma_{ZZ}}\right)^2 + \left(\frac{N-\overline{N}}{\sigma_{NN}}\right)^2 - 2\rho\left(\frac{Z-\overline{Z}}{\sigma_{ZZ}}\right)\left(\frac{N-\overline{N}}{\sigma_{NN}}\right)\right], \quad (13)$$

where $\rho = \sigma_{NZ}^2/\sigma_{ZZ}\sigma_{NN}$ is the correlation coefficient. The mean values $\overline{N}$, $\overline{Z}$ are the mean neutron and proton numbers of the target-like or project-like fragments.

III. TRANSPORT COEFFICIENTS FOR NUCLEON EXCHANGE

A. Quantal diffusion coefficients

The quantal expressions of the proton and neutron diffusion coefficients are determined by the correlation function of the stochastic part of the drift coefficients according to [46,47],

$$D_{\alpha\alpha}(t) = \int_0^t dt' \overline{\delta v_\alpha^\lambda(t)\delta v_\alpha^\lambda(t')}. \quad (14)$$

From Eq. (4), the stochastic parts of the drift coefficients are given by

$$\delta v_\alpha^\lambda(t) = \frac{\hbar}{m}\sum_{ij\in\alpha}\int d^3r g(x)\mathrm{Im}(\Phi_j^*(\vec{r},t)\nabla_x\Phi_i(\vec{r},t))\delta\rho_{ji}^\lambda. \quad (15)$$

In determining the stochastic part of the drift coefficients, we impose a physical constraint on the summations of single-particle sates. The transitions among single particle states originating from projectile or target nuclei do not contribute to nucleon exchange mechanism. Therefore, in this expression, we restrict the summations as follows: when the summation $i \in T$ runs over the states originating from target nucleus, the summation $j \in P$ runs over the states originating from the projectile, and vice versa.

Using the basic postulate of the SMF approach given by Eq. (5), it is possible to calculate the correlation functions of the stochastic part of the drift coefficients, and hence we can determine the quantal expression for the diffusion coefficients. The correlation function involves a complete set of time-dependent particle and hole states. The standard solutions of TDHF give the time-dependent wave functions

of the occupied hole states. The solution of complete set of time-dependent particle states requires a very large amount of effort. However, it is possible to eliminate the complete set of particle states by employing closure relation with the help of a reasonable approximation. We recognize that the time-dependent single-particle wave functions obtained from the TDHF exhibit nearly a diabatic behavior [54]. In other words, during short time intervals the nodal structure of time-dependent wave functions do not change appreciably. The most dramatic diabatic behavior of the time-dependent wave functions is apparent in the fission dynamics. The Hartree-Fock solutions force the system to follow the diabatic path, which prevents the system to break up into fragments. As a result of these observations, we introduce, during short time $\tau = t - t'$ evolutions in the order of the correlation time, a diabatic approximation into the time-dependent wave functions by shifting the time backward (or forward) according to

$$\Phi_a(\vec{r},t') \approx \Phi_a(\vec{r} - \vec{u}\tau,t), \tag{16}$$

where $\vec{u}$ denotes a suitable flow velocity of nucleons. Now, we can employ the closure relation

$$\sum_a \Phi_a^*(\vec{r}_1,t)\Phi_a(\vec{r}_2,t') \approx \sum_a \Phi_a^*(\vec{r}_1,t)\Phi_a(\vec{r}_2 - \vec{u}\tau,t) = \delta(\vec{r}_1 - \vec{r}_2 + \vec{u}\tau), \tag{17}$$

where summation a runs over the complete set of states originating from target or projectile, and the closure relation is valid for each set of the spin-isospin degrees of freedom. We note that diabatic approximation is not determined with a single flow velocity. As seen from Eq. (19) of Ref. [48], when the closure relation is employed over the complete set of states originating from the projectile, the flow velocity is taken as the flow velocity of each hole state originating from target, and similarly when the closure relation is employed for the complete set of states originating from target, the flow velocity is taken as the flow velocity of each hole state originating from target. Consequently, the main contribution to nucleon diffusion arises from the nucleon exchanges around the Fermi surface. Carrying out an algebraic manipulation, we find that the quantal expressions of the proton and neutron diffusion coefficients are given by

$$\begin{aligned} D_{\alpha\alpha}(t) = & \int_0^t d\tau G_0(\tau) \int d^3r \tilde{g}(x) \\ & \times \left[J_\alpha^T(\vec{r},t-\tau/2) + J_\alpha^P(\vec{r},t-\tau/2)\right] \\ & - \int_0^t d\tau \mathrm{Re}\Bigg[\sum_{h'\in P,h\in T} A_{h'h}^\alpha(t)A_{h'h}^{*\alpha}(t-\tau) \\ & + \sum_{h'\in T,h\in P} A_{h'h}^\alpha(t)A_{h'h}^{*\alpha}(t-\tau)\Bigg], \end{aligned} \tag{18}$$

where $\tilde{g}(x) = (1/\sqrt{\pi}\kappa)\exp[-(x/\kappa)^2]$. The quantity $J_\alpha^T(\vec{r},t - \tau/2)$ represents the sum of magnitude of the current densities due to hole wave functions originating from target nuclei,

$$J_\alpha^T(\vec{r},t) = \frac{\hbar}{m}\sum_{h\in T} |\mathrm{Im}(\Phi_h^*(\vec{r},t)\nabla_x\Phi_h(\vec{r},t))|. \tag{19}$$

Here, the quantity $G_0(\tau) = [1/(\tau_0\sqrt{4\pi})]\exp[-(\tau/2\tau_0)^2]$ denotes the memory kernel with the memory time given by $\tau_0 = \kappa/|u_0|$ with $u_0 = \langle u_h\rangle$ as the average flow speed of hole states across the window. The quantity $J_\alpha^P(\vec{r},t-\tau/2)$ associated with the projectile states is given by a similar expression. The hole-hole matrix elements $A_{h'h}^\alpha(t)$ calculated with the wave functions originating from projectile and target nuclei are given by

$$\begin{aligned} A_{h'h}^\alpha(t) = \frac{\hbar}{2m}\int d^3r g(x)\big[&\Phi_{h'}^{*\alpha}(\vec{r},t)\nabla_x\Phi_h^\alpha(\vec{r},t) \\ &- \Phi_h^\alpha(\vec{r},t)\nabla_x\Phi_{h'}^{*\alpha}(\vec{r},t)\big]. \end{aligned} \tag{20}$$

For a detailed derivation of quantal diffusion coefficients Eq. (18) and definition of flow velocities, we refer the reader to Ref. [48]. There is a close analogy between the quantal expression and the classical diffusion coefficient in a random walk problem [46,47,55]. The first line in the quantal expression gives the sum of the nucleon currents from the target-like fragment to the projectile-like fragment and from the projectile-like fragment to the target-like fragment, which is integrated over the memory. This is analogous to the random walk problem, in which the diffusion coefficient is given by the sum of the rate for the forward and backward steps. The second line in the quantal diffusion expression stands for the Pauli blocking effects in nucleon transfer mechanism, which does not have a classical counterpart. It is important to note that the quantal diffusion coefficients are entirely determined in terms of the occupied single-particle wave functions obtained from the TDHF solutions. The quantal diffusion coefficients contain the effects of the shell structure, take into account full collision geometry and do not involve any free parameters. In the collisions at the energies we considered, the average value of nucleon flow speed across the window is $u_0 \approx 0.05c$ [48], which gives a memory time around $\tau_0 = \kappa/u_0 \approx 20$ fm/c. Since the memory time is much shorter than a typical interaction time of collisions, $\tau_0 << 500$ fm/c, the memory effect is not very effective in nucleon exchange mechanism. Consequently, we can neglect the τ dependence in the current densities in Eq. (18), carry out the τ integration over the memory kernel to give $\int_0^t G_0(\tau)d\tau \approx 1/2$. Because of the same reason, memory effect is not very effective in the Pauli blocking terms as well, however in the calculations we keep the memory integrals in these terms.

B. Nucleon drift coefficients

In order to solve covariances from Eqs. (9)–(11), in addition to the diffusion coefficients D_{ZZ} and D_{NN}, we need to know the rate of change of drift coefficients in the vicinity of their mean values. According to the SMF approach, in order to calculate rates of the drift coefficients, we should calculate neighboring events in the vicinity of the mean-field event. Here, instead of such a detailed description, we employ the fluctuation-dissipation theorem, which provides a general

relation between the diffusion and drift coefficients in the transport mechanism of the relevant collective variables as described in the phenomenological approaches [55]. Proton and neutron diffusions in the N-Z plane are driven in a correlated manner by the potential energy surface of the dinuclear system. As a consequence of the symmetry energy, the diffusion in direction perpendicular to the β-stability valley takes place rather rapidly leading to a fast equilibration of the charge asymmetry, and diffusion continues rather slowly along the β-stability valley. Borrowing an idea from Refs. [54,56], we parametrize the N_1 and Z_1 dependence of the potential energy surface of the dinuclear system in terms of two parabolic forms:

$$U(N_1,Z_1) = \tfrac{1}{2}a(z\cos\theta - n\sin\theta)^2 + \tfrac{1}{2}b(z\sin\theta + n\cos\theta)^2. \quad (21)$$

Here, $z = Z_0 - Z_1$, $n = N_0 - N_1$, and θ denotes the angle between β-stability valley and the N axis in the N-Z plane. The quantities N_0 and Z_0 denote the equilibrium values of the neutron and proton numbers, which are approximately determined by the average values of the neutron and proton numbers of the projectile and target ions, $N_0 = (N_P + N_T)/2$ and $Z_0 = (Z_P + Z_T)/2$. The first term in this expression describes a strong driving force perpendicular to the β-stability valley, while the second term describes a relative weak driving force toward symmetry along the valley. In symmetric collisions, N_0 and Z_0 are equal to the initial neutron and proton numbers of the target or projectile nuclei. Following from the fluctuation-dissipation theorem, it is possible to relate the proton and neutron drift coefficients to the diffusion coefficients and the associated driving forces, in terms of the Einstein relations as follows [54,56]:

$$\begin{aligned} v_n &= -\frac{D_{NN}}{T}\frac{\partial U}{\partial N_1} = +\frac{D_{NN}}{T}\frac{\partial U}{\partial n} \\ &= D_{NN}[-\alpha\sin\theta(z\cos\theta - n\sin\theta) \\ &\quad + \beta\cos\theta(z\sin\theta + n\cos\theta)] \end{aligned} \quad (22)$$

and

$$\begin{aligned} v_z &= -\frac{D_{ZZ}}{T}\frac{\partial U}{\partial Z_1} = +\frac{D_{ZZ}}{T}\frac{\partial U}{\partial z} \\ &= D_{ZZ}[+\alpha\cos\theta(z\cos\theta - n\sin\theta) \\ &\quad + \beta\sin\theta(z\sin\theta + n\cos\theta)]. \end{aligned} \quad (23)$$

Here, the temperature T is absorbed into coefficients α and β, consequently temperature does not appear as a parameter in the description. In asymmetric collisions, it is possible to determine α and β by matching the mean values of neutron and proton drift coefficients obtained from the TDHF solutions. In symmetric collisions, the mean value of drift coefficients are zero and the mean values of neutron and proton numbers do not change and remain equal to their initial values. Therefore it is not possible to determine the coefficients α and β from the full TDHF solutions. However, we can determine these coefficients employing the one-sided neutron and proton fluxes from projectile-like fragment to the target-like fragment or vice versa. We indicate neutron and proton numbers of one of the fragments as $\tilde{N}_1$ and $\tilde{Z}_1$. Then, the neutron and proton numbers of this fragment monotonically decreases according to

$$\begin{aligned} \frac{d}{dt}\begin{pmatrix}\tilde{Z}_1(t)\\ \tilde{N}_1(t)\end{pmatrix} &= \int d^3r g(x)\begin{pmatrix}\tilde{J}_p(\vec{r},t)\\ \tilde{J}_n(\vec{r},t)\end{pmatrix} \\ &= \begin{pmatrix}\tilde{v}_p(t)\\ \tilde{v}_n(t)\end{pmatrix}. \end{aligned} \quad (24)$$

Here, $\tilde{v}_\alpha(t)$ with $\alpha = n,p$ denotes the one-sided neutron and proton drift coefficients towards the other fragment and the one-sided current density $\tilde{J}_\alpha(\vec{r},t)$ is given by Eq. (7) keeping only negative terms in the summation over the hole states. The one-sided drift coefficients $\tilde{v}_n$ and $\tilde{v}_p$ are related to the driving force with the similar expressions given by Eqs. (22) and (23), except that n and z are replaced by $\tilde{n} = N_0 - \tilde{N}_1$ and $\tilde{z} = Z_0 - \tilde{Z}_1$ and by including an overall sign change

$$\begin{aligned} \tilde{v}_n &= D_{NN}[+\alpha\sin\theta(\tilde{z}\cos\theta - \tilde{n}\sin\theta) \\ &\quad - \beta\cos\theta(\tilde{z}\sin\theta + \tilde{n}\cos\theta)] \end{aligned} \quad (25)$$

and

$$\begin{aligned} \tilde{v}_z &= D_{ZZ}[-\alpha\cos\theta(\tilde{z}\cos\theta - \tilde{n}\sin\theta) \\ &\quad - \beta\sin\theta(\tilde{z}\sin\theta + \tilde{n}\cos\theta)]. \end{aligned} \quad (26)$$

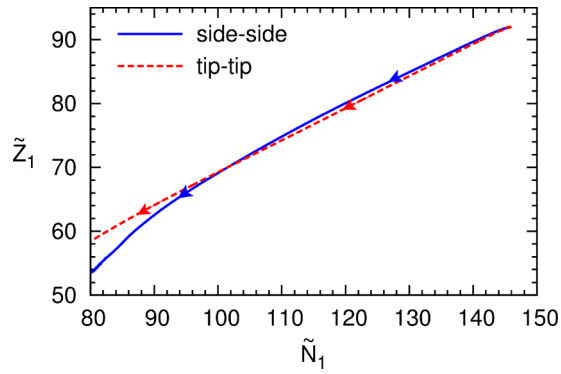

FIG. 2. Mean drift path of the projectile-like fragments in the N-Z plane in the central collisions of $^{238}\mathrm{U} + ^{238}\mathrm{U}$ at side-side collision with energy $E_{\mathrm{c.m.}} = 900$ MeV (solid line), and at tip-tip collision with energy $E_{\mathrm{c.m.}} = 1050$ MeV (dashed line), obtained with one-sided flux in TDHF calculations.

Figure 2 shows the one-sided mean-drift paths of projectile-like fragments which are determined by keeping the one-sided neutron and proton fluxes from projectile-like to the target-like fragments in the side-side and tip-tip collisions of $^{238}\mathrm{U} + ^{238}\mathrm{U}$. Using this information, we can extract the angle θ and the magnitude of coefficients α and β. We find that the angle between the mean one-sided drift path and N axis is about $\theta \approx 30^\circ$ in both collision geometries. As a result of the quantal effects arising mainly from the shell structure, we observe that the coefficients α and β exhibit fluctuations as a function of time. In the side-side collision, during the relevant time interval from 200 fm/c to 800 fm/c, the average values of these coefficients are about $\alpha \approx 0.035$ and $\beta \approx 0.007$. In the tip-tip collision, during the relevant time interval from 200 fm/c to 700 fm/c, the average values of these coefficients are

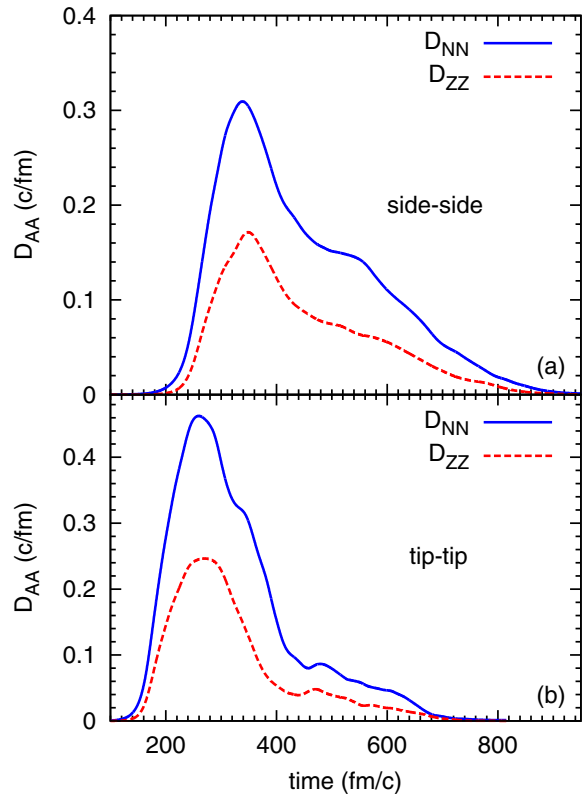

FIG. 3. Neutron and proton diffusion coefficients in the central collisions of $^{238}\mathrm{U} + ^{238}\mathrm{U}$ (a) side-side collision with energy $E_{\mathrm{c.m.}} = 900$ MeV, and (b) tip-tip collision with energy $E_{\mathrm{c.m.}} = 1050$ MeV, respectively.

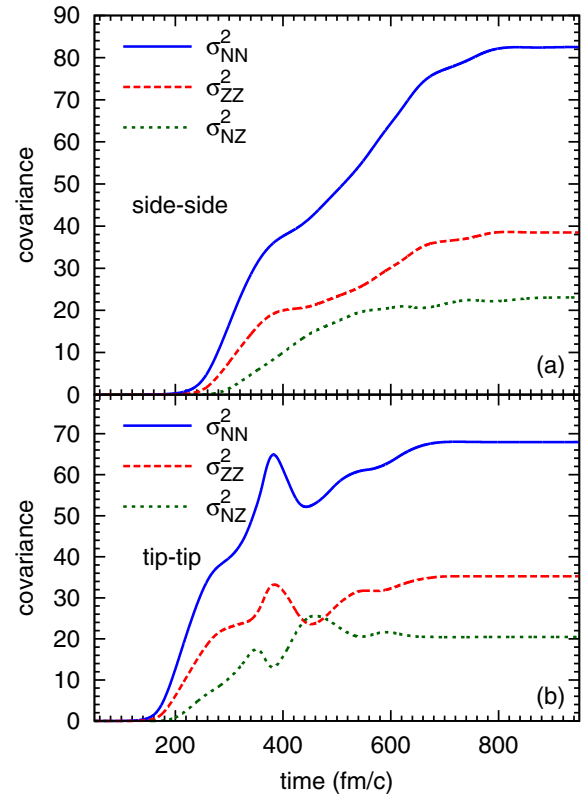

FIG. 4. Neutron, proton covariances in the central collisions of $^{238}\mathrm{U} + ^{238}\mathrm{U}$ (a) side-side collision with energy $E_{\mathrm{c.m.}} = 900$ MeV, and (b) tip-tip collision with energy $E_{\mathrm{c.m.}} = 1050$ MeV, respectively.

about $\alpha \approx 0.039$ and $\beta \approx 0.009$. These results are consistent with the potential energy surface of the liquid drop picture. The potential energy surface in the $(N\text{-}Z)$ plane has a steeply rising parabolic shape in the perpendicular direction to the stability valley and has a shallow behavior along the stability valley. Because of a simple analytical structure, we can easily calculate derivatives of drift coefficients which are needed in differential Eqs. (9)–(11) for determining the covariances.

IV. PRIMARY FRAGMENT DISTRIBUTIONS

In determining the primary fragment distributions, the main input quantities are the neutron and proton diffusions coefficients given in Eq. (18). The diffusion coefficients are entirely determined by the occupied time-dependent single-particle states. The TDHF theory includes the one-body dissipation mechanism. We can use the same information provided by the TDHF to calculate the diffusion coefficients which describe the fluctuation mechanism of the collective motion. The reason behind this fact is the fundamental relation that exists between dissipation and fluctuation mechanism of the collective motion as stated in the fluctuation-dissipation theorem [46,47]. Figure 3 shows the neutron (solid lines) and proton (dashed lines) diffusion coefficients in the side-side and the tip-tip central collisions of $^{238}\mathrm{U} + ^{238}\mathrm{U}$ at bombarding energies $E_{\mathrm{c.m.}} = 900$ MeV and $E_{\mathrm{c.m.}} = 1050$ MeV, respectively. We determine the proton, neutron covariance by solving the coupled differential Eqs. (9)–(11) with the initial conditions $\sigma_{nn}(0) = 0$, $\sigma_{pp}(0) = 0$ and $\sigma_{np}(0) = 0$. Figure 4 illustrates these covariance as a function of time in the side-side and the tip-tip central collisions of $^{238}\mathrm{U} + ^{238}\mathrm{U}$. Primary fragment distribution in the $N\text{-}Z$ plane is determined by a correlated Gaussian given by Eq. (12). The elliptic curves in Fig. 5 show equal probability lines relative to the center point for producing fragments for three values of the exponent $C = 0.5$, 1.0, 1.5 in the Gaussian function. For example the probability for producing fragments on the ellipse with $C = 0.5$ relative to the symmetric fragmentation is $\exp(-0.5) = 0.6$. Primary fragment distributions have a similar behavior in both side-side and tip-tip collisions as seen from panels (a) and (b). The variance of fragment mass distributions is determined by

$$\sigma^2_{AA}(t) = \sigma^2_{NN}(t) + \sigma^2_{ZZ}(t) + 2\sigma^2_{NZ}(t). \tag{27}$$

As seen from Fig. 4, at the end of the final states of collisions the covariances of the fragment mass distribution have the values $\sigma_{AA}(t) = 12.9$ and $\sigma_{AA}(t) = 12.0$ in side-side and tip-tip collisions, respectively. Figure 6 illustrates the Gaussian form of the mass distributions of the primary fragments with a mean value $\overline{A} = 238$ and variances $\sigma_{AA}(t) = 12.9$ and $\sigma_{AA}(t) = 12.0$.

In the symmetric fragmentation of the final state, we can determine the excitation energy of each final $^{238}\mathrm{U}$ nucleus

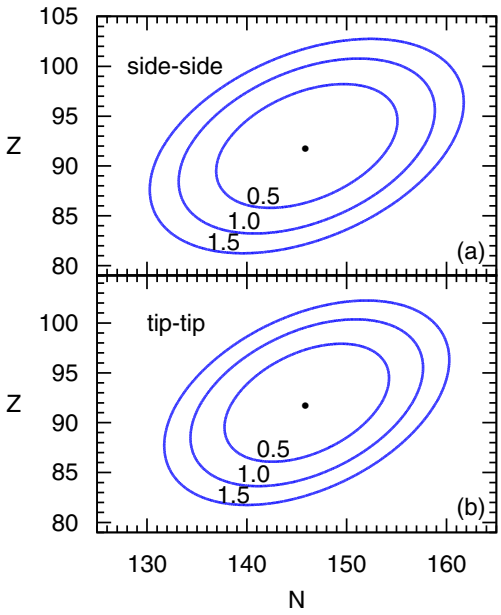

FIG. 5. Equal probability lines for primary fragment formation with $C = 0.5, 1.0, 1.5$ in the central collisions of $^{238}\mathrm{U} + ^{238}\mathrm{U}$ (a) side-side collision with energy $E_{\mathrm{c.m.}} = 900$ MeV, and (b) tip-tip collision with energy $E_{\mathrm{c.m.}} = 1050$ MeV, respectively.

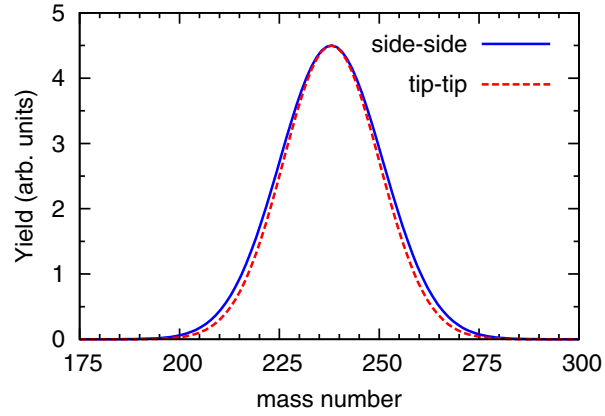

FIG. 6. Primary fragment mass distributions in the central collisions of $^{238}\mathrm{U} + ^{238}\mathrm{U}$ at side-side collision with energy $E_{\mathrm{c.m.}} = 900$ MeV (solid line) and at tip-tip collision with energy $E_{\mathrm{c.m.}} = 1050$ MeV (dashed line).

by calculating the final total kinetic energy (TKE) from the TDHF solutions. We find TKE = 620 MeV and TKE = 634 MeV in the side-side and the tip-tip collisions, respectively. From the energy conservation, $E^* = E_{\mathrm{c.m.}} - \mathrm{TKE}$, we find that the excitation energy of each ^{238}U nucleus is $E^* = 140$ MeV and $E^* = 208$ MeV, in the side-side and the tip-tip collisions. As a result of multinucleon transfer in the collisions, there are many binary fragments in the final state as indicated in distributions in Fig. 5. In the present work, we cannot calculate the excitation energies of each final fragment pair, but we can estimate them by using the Viola systematics. It is very reasonable to assume that all available initial relative kinetic energy is dissipated into the internal excitations and is shared between the fragments in proportion to the ratio of masses in possible final binary channel. According to the Viola formula, total excitation E_c^* in a binary channel is determined by $E_c^* = E_{\mathrm{c.m.}} + Q_c - (\mathrm{TKE})_c$. Here, Q_c is the Q value of the binary channel and $(\mathrm{TKE})_c$ indicates the total final kinetic energy of fragments. $(\mathrm{TKE})_c$ is approximately determined by Coulomb potential energy of the binary fragments at an effective relative distance determined by an adjustable parameter r_0 as

$$(\mathrm{TKE})_c = \frac{1}{4\pi\varepsilon_0}\frac{Z_{1c}Z_{2c}e^2}{r_0\left(A_{1c}^{1/3} + A_{2c}^{1/3}\right)}. \tag{28}$$

With help of the TKE of the symmetric binary channel, we adjust the parameter $r_0 = 1.59$ fm and $r_0 = 1.55$ fm for the side-side and tip-tip collisions, respectively. We estimate that primary fragments inside the elliptic region with $C = 1.5$ have excitation energies in the range of (120–150) MeV and (185–225) MeV in the side-side and tip-tip collisions, respectively. In this work, we carry out primary charge and mass distributions of fragments, which have rather large dispersions. These primary fragments are highly excited. Highly excited intermediate fragments cool down by particle evaporation and heavy fragments should immediately fission. Therefore the secondary charge and mass distributions are expected to have smaller dispersions. However, we do not perform de-excitation calculations of the primary fragments in this work. In a recent work, a different analysis of a multinucleon transfer mechanism in $^{238}\mathrm{U} + ^{238}\mathrm{U}$ collisions were carried out by Zhao *et al.* [4] by employing improved quantal molecular dynamics (ImQMD) simulations. In this work, authors report the cross sections for production of primary fragments as well as the secondary fragment distributions. Indeed dispersions of the mass and charge distributions are reduced by de-excitation of the primary fragments. In the ImQMD simulation a simplified version of the Skyrme interaction was employed, the Pauli blocking effect is treated in the semiclassical approximation and calculation are carried out for a range of impact parameters. On the other hand, in the quantal calculations presented in the present work, the full Skyrme interaction is employed and the Pauli blocking effect is exactly taken into account. Since in the calculations presented here are carried out only in the central geometry, a detail comparison of the result with the result reported with molecular dynamics simulation for the primary fragment distribution is not possible. From Fig. 1 of Ref. [4], it appears that the dispersion of the charge and mass distribution of the primary fragment distribution is smaller than the quantal calculations presented here. In collisions with finite impact parameters, the interaction times are much shorter than the interaction time in the central collisions. Shorter interaction times leads to smaller dispersion in the primary fragment distributions. We believe that smaller dispersions reported in the molecular dynamics calculations, among the other reasons, are the results of simulations carried out with finite impact parameters.

V. CONCLUSIONS

The SMF approach improves the standard mean-field description by incorporating thermal and quantal fluctuations in the collective motion. The approach requires to generate an ensemble of mean field trajectories. The initial conditions for the events in the ensemble are specified by the quantal and thermal fluctuations in the initial state in a suitable manner, and each event is evolved by its own self-consistent mean-field Hamiltonian. In reactions where the colliding system maintains a dinuclear structure, the reaction dynamics can be described in terms of a set of relevant macroscopic variables, which can be defined with the help of the window dynamics. The SMF approach gives rise to a quantal Langevin description for the evolution of the macroscopic variables. In this work, we apply this approach and analyze multinucleon transfer mechanism in the central collisions of $^{238}\mathrm{U} + ^{238}\mathrm{U}$ in side-side geometry with energy $E_{\mathrm{c.m.}} = 900$ MeV and in tip-tip geometry with energy $E_{\mathrm{c.m.}} = 1050$ MeV. Fluctuation mechanism of neutron and proton exchanges is described by the quantal diffusion coefficients. Quantal diffusion coefficients are entirely determined by the single-particle states of the TDHF equations. These coefficients include the full geometry of the collision process and the effect of the shell structure. They do not involve any adjustable parameters and do not require any additional information. Deep underlying reason behind this is the fact that the dissipation and fluctuation aspects of the dynamics are connected according to the fluctuation-dissipation theorem of nonequilibrium statistical mechanics. We estimate the excitation energies of the primary fragments with the help of Viola formula which provides an approximate description of the total final kinetic energy of the binary fragments. The highly excited fragments are cooled down by particle emission and in particular highly excited heavy fragments are expected to decay rapidly by fission. We plan to carry out de-excitation calculations and determine the secondary fragment distributions in a subsequent work.

ACKNOWLEDGMENTS

S.A. gratefully acknowledges the IPN-Orsay and the Middle East Technical University for warm hospitality extended to him during his visits. S.A. also gratefully acknowledges useful discussions with D. Lacroix, and is very much thankful to F. Ayik for continuous support and encouragement. This work is supported in part by US DOE Grants No. DE-SC0015513 and No. DE-SC0013847.

[1] G. G. Adamian, N. V. Antonenko, and W. Scheid, Characteristics of quasifission products within the dinuclear system model, Phys. Rev. C **68**, 034601 (2003).
[2] V. Zagrebaev and W. Greiner, Shell effects in damped collisions: A new way to superheavies, J. Phys. G **34**, 2265 (2007).
[3] Y. Aritomo, Analysis of dynamical processes using the mass distribution of fission fragments in heavy-ion reactions, Phys. Rev. C **80**, 064604 (2009).
[4] K. Zhao, Z. Li, Y. Zhang, N. Wang, Q. Li, C. Shen, Y. Wang, and X. Wu, Production of unknown neutron-rich isotopes in $^{238}\mathrm{U} + ^{238}\mathrm{U}$ collisions at near-barrier energy, Phys. Rev. C **94**, 024601 (2016).
[5] J. W. Negele, The mean-field theory of nuclear-structure and dynamics, Rev. Mod. Phys. **54**, 913 (1982).
[6] T. Nakatsukasa, K. Matsuyanagi, M. Matsuo, and K. Yabana, Time-dependent density-functional description of nuclear dynamics, Rev. Mod. Phys. **88**, 045004 (2016).
[7] C. Simenel, Nuclear quantum many-body dynamics, Eur. Phys. J. A **48**, 152 (2012).
[8] C. Golabek and C. Simenel, Collision Dynamics of Two $^{238}\mathrm{U}$ Atomic Nuclei, Phys. Rev. Lett. **103**, 042701 (2009).
[9] D. J. Kedziora and C. Simenel, New inverse quasifission mechanism to produce neutron-rich transfermium nuclei, Phys. Rev. C **81**, 044613 (2010).
[10] C. Simenel, D. J. Hinde, R. du Rietz, M. Dasgupta, M. Evers, C. J. Lin, D. H. Luong, and A. Wakhle, Influence of entrance-channel magicity and isospin on quasi-fission, Phys. Lett. B **710**, 607 (2012).
[11] A. Wakhle, C. Simenel, D. J. Hinde, M. Dasgupta, M. Evers, D. H. Luong, R. du Rietz, and E. Williams, Interplay Between Quantum Shells and Orientation in Quasifission, Phys. Rev. Lett. **113**, 182502 (2014).
[12] V. E. Oberacker, A. S. Umar, and C. Simenel, Dissipative dynamics in quasifission, Phys. Rev. C **90**, 054605 (2014).
[13] K. Hammerton, Z. Kohley, D. J. Hinde, M. Dasgupta, A. Wakhle, E. Williams, V. E. Oberacker, A. S. Umar, I. P. Carter, K. J. Cook, J. Greene, D. Y. Jeung, D. H. Luong, S. D. McNeil, C. S. Palshetkar, D. C. Rafferty, C. Simenel, and K. Stiefel, Reduced quasifission competition in fusion reactions forming neutron-rich heavy elements, Phys. Rev. C **91**, 041602(R) (2015).
[14] A. S. Umar and V. E. Oberacker, Time-dependent HF approach to SHE dynamics, Nucl. Phys. A **944**, 238 (2015).
[15] A. S. Umar, V. E. Oberacker, and C. Simenel, Shape evolution and collective dynamics of quasifission in the time-dependent Hartree-Fock approach, Phys. Rev. C **92**, 024621 (2015).
[16] K. Sekizawa and K. Yabana, Time-dependent Hartree-Fock calculations for multinucleon transfer and quasifission processes in the $^{64}\mathrm{Ni} + ^{238}\mathrm{U}$ reaction, Phys. Rev. C **93**, 054616 (2016).
[17] A. S. Umar, V. E. Oberacker, and C. Simenel, Fusion and quasifission dynamics in the reactions $^{48}\mathrm{Ca} + ^{249}\mathrm{Bk}$ and $^{50}\mathrm{Ti} + ^{249}\mathrm{Bk}$ using a time-dependent Hartree-Fock approach, Phys. Rev. C **94**, 024605 (2016).
[18] C. Simenel and A. S. Umar, Formation and dynamics of fission fragments, Phys. Rev. C **89**, 031601(R) (2014).
[19] G. Scamps, C. Simenel, and D. Lacroix, Superfluid dynamics of $^{258}\mathrm{Fm}$ fission, Phys. Rev. C **92**, 011602(R) (2015).
[20] C. Simenel, G. Scamps, D. Lacroix, and A. S. Umar, Superfluid fission dynamics with microscopic approaches, EPJ Web. Conf. **107**, 07001 (2016).
[21] P. M. Goddard, P. D. Stevenson, and A. Rios, Fission dynamics within time-dependent Hartree-Fock: Deformation-induced fission, Phys. Rev. C **92**, 054610 (2015).
[22] P. M. Goddard, P. D. Stevenson, and A. Rios, Fission dynamics within time-dependent Hartree-Fock. II. Boost-induced fission, Phys. Rev. C **93**, 014620 (2016).

[23] A. Bulgac, P. Magierski, K. J. Roche, and I. Stetcu, Induced Fission of ^{240} Pu Within a Real-Time Microscopic Framework, Phys. Rev. Lett. **116**, 122504 (2016).

[24] A. S. Umar and V. E. Oberacker, Three-dimensional unrestricted time-dependent Hartree-Fock fusion calculations using the full Skyrme interaction, Phys. Rev. C **73**, 054607 (2006).

[25] J. A. Maruhn, P.-G. Reinhard, P. D. Stevenson, and A. S. Umar, The TDHF code Sky3D, Comput. Phys. Commun. **185**, 2195 (2014).

[26] B. Schuetrumpf, W. Nazarewicz, and P.-G. Reinhard, Time-dependent density functional theory with twist-averaged boundary conditions, Phys. Rev. C **93**, 054304 (2016).

[27] S. E. Koonin, K. T. R. Davies, V. Maruhn-Rezwani, H. Feldmeier, S. J. Krieger, and J. W. Negele, Time-dependent Hartree-Fock calculations for ^{16}O $+^{16}$O and ^{40}Ca $+$ ^{40}Ca reactions, Phys. Rev. C **15**, 1359 (1977).

[28] C. Simenel, Particle Transfer Reactions with the Time-Dependent Hartree-Fock Theory Using a Particle Number Projection Technique, Phys. Rev. Lett. **105**, 192701 (2010).

[29] K. Sekizawa and K. Yabana, Time-dependent Hartree-Fock calculations for multinucleon transfer processes in ^{40,48}Ca $+$ ^{124}Sn, ^{40}Ca $+$ ^{208}Pb, and ^{58}Ni $+$ ^{208}Pb reactions, Phys. Rev. C **88**, 014614 (2013).

[30] G. Scamps and D. Lacroix, Effect of pairing on one- and two-nucleon transfer below the Coulomb barrier: A time-dependent microscopic description, Phys. Rev. C **87**, 014605 (2013).

[31] K. Sekizawa and K. Yabana, Particle-number projection method in time-dependent Hartree-Fock theory: Properties of reaction products, Phys. Rev. C **90**, 064614 (2014).

[32] S. Kazuyuki and Y. Kazuhiro, Time-dependent Hartree–Fock calculations for multi-nucleon transfer processes: Effects of particle evaporation on production cross sections, EPJ Web of Conf. **86**, 00043 (2015).

[33] C. H. Dasso, T. Dossing, and H. C. Pauli, On the mass distribution in time-dependent Hartree-Fock calculations of heavy-ion collisions, Z. Phys. A **289**, 395 (1979).

[34] C. Simenel, Particle-Number Fluctuations and Correlations in Transfer Reactions Obtained Using the Balian-Vénéroni Variational Principle, Phys. Rev. Lett. **106**, 112502 (2011).

[35] R. Balian and M. Vénéroni, Correlations and fluctuations in static and dynamic mean-field approaches, Ann. Phys. (NY) **216**, 351 (1992).

[36] H. Goutte, J. F. Berger, P. Casoli, and D. Gogny, Microscopic approach of fission dynamics applied to fragment kinetic energy and mass distributions in ^{238}U, Phys. Rev. C **71**, 024316 (2005).

[37] S. Ayik, A stochastic mean-field approach for nuclear dynamics, Phys. Lett. B **658**, 174 (2008).

[38] M. Tohyama, Two-body collision effects on the low-L fusion window in ^{16}O $+$ ^{16}O reactions, Phys. Lett. B **160**, 235 (1985).

[39] M. Tohyama and A. S. Umar, Quadrupole resonances in unstable oxygen isotopes in time-dependent density-matrix formalism, Phys. Lett. B **549**, 72 (2002).

[40] M. Assié and D. Lacroix, Probing Neutron Correlations Through Nuclear Breakup, Phys. Rev. Lett. **102**, 202501 (2009).

[41] M. Tohyama and A. S. Umar, Two-body dissipation effects on the synthesis of superheavy elements, Phys. Rev. C **93**, 034607 (2016).

[42] S. Ayik, B. Yilmaz, and O. Yilmaz, Multinucleon exchange in quasifission reactions, Phys. Rev. C **92**, 064615 (2015).

[43] D. Lacroix and S. Ayik, Stochastic quantum dynamics beyond mean field, Eur. Phys. J. A **50**, 95 (2014).

[44] B. Yilmaz, S. Ayik, D. Lacroix, and O. Yilmaz, Nucleon exchange in heavy-ion collisions within a stochastic mean-field approach, Phys. Rev. C **90**, 024613 (2014).

[45] Y. Tanimura, D. Lacroix, and S. Ayik, Microscopic Phase-Space Exploration Modeling of ^{258}Fm Spontaneous Fission, Phys. Rev. Lett. **118**, 152501 (2017).

[46] C. W. Gardiner, *Quantum Noise* (Springer-Verlag, Berlin, 1991).

[47] U. Weiss, *Quantum Dissipative Systems*, 2nd ed. (World Scientific, Singapore, 1999).

[48] S. Ayik, O. Yilmaz, B. Yilmaz, and A. S. Umar, Quantal nucleon diffusion: Central collisions of symmetric nuclei, Phys. Rev. C **94**, 044624 (2016).

[49] A. S. Umar, M. R. Strayer, J. S. Wu, D. J. Dean, and M. C. Güçlü, Nuclear Hartree-Fock calculations with splines, Phys. Rev. C **44**, 2512 (1991).

[50] K.-H. Kim, T. Otsuka, and P. Bonche, Three-dimensional TDHF calculations for reactions of unstable nuclei, J. Phys. G **23**, 1267 (1997).

[51] W. U. Schröder, J. R. Huizenga, and J. Randrup, Correlated mass and charge transport induced by statistical nucleon exchange in damped nuclear reactions, Phys. Lett. B **98**, 355 (1981).

[52] A. C. Merchant and W. Nörenberg, Neutron and proton diffusion in heavy-ion collisions, Phys. Lett. B **104**, 15 (1981).

[53] H. Risken and T. Frank, *The Fokker-Planck Equation* (Springer-Verlag, Berlin, 1996).

[54] W. Nörenberg, Memory effects in the energy dissipation for slow collective nuclear motion, Phys. Lett. B **104**, 107 (1981).

[55] J. Randrup, Theory of transfer-induced transport in nuclear collisions, Nucl. Phys. A **327**, 490 (1979).

[56] A. C. Merchant and W. Nörenberg, Microscopic transport theory of heavy-ion collisions, Z. Phys. A **308**, 315 (1982).